INVITED PAPER

PACS numbers: 28.60.+s; 42.62.Cf
DOI: 10.1070/QE2005v035n10ABEH006601

Development of the laser isotope separation method (AVLIS) for obtaining weight amounts of highly enriched ^{150}Nd isotope

A.P. Babichev, I.S. Grigoriev, A.I. Grigoriev, A.P. Dorovskii, A.B. D'yachkov, S.K. Kovalevich, V.A. Kochetov, V.A. Kuznetsov, V.P. Labozin, A.V. Matrakhov, S.M. Mironov, S.A. Nikulin, A.V. Pesnya, N.I. Timofeev, V.A. Firsov, G.O. Tsvetkov, G.G. Shatalova

Contents

***Abstract*. Results obtained at the first stage of development of the experimental technique for obtaining weight amounts of the highly enriched ^{150}Nd isotope by laser photoionisation are presented. The vaporiser and the laser are designed, and various methods of irradiation of neodymium vapour and extraction of photoions are tested. The product yield ~ 40 mg h^{-1} for the ~ 60 % enrichment and 25 mg h^{-1} for the ~ 65 % enrichment is achieved for a vaporiser of length 27 cm. The cost of constructing the facility for preparing 50 kg of the ^{150}Nd isotope, intended for determining the neutrino mass, is estimated. This estimate shows that the cost of production can be lowered by a factor of 5 – 7 compared to the electromagnetic method.**

A.P. Babichev, I.S. Grigoriev, A.I. Grigoriev, A.P. Dorovskii, A.B. D'yachkov, S.K. Kovalevich, V.A. Kochetov, V.A. Kuznetsov, V.P. Labozin, A.V. Matrakhov, S.M. Mironov, S.A. Nikulin, A.V. Pesnya, N.I. Timofeev, V.A. Firsov, G.O. Tsvetkov, G.G. Shatalova Russian Research Centre Kurchatov Institute, pl. akad. Kurchatova 1, 123182 Moscow, Russia; e-mail: flash@imp.kiae.ru

Received 25 March 2005; revision received 18 August 2005
Kvantovaya Elektronika **35** (10) 879 – 890 (2005)
Translated by Ram Wadhwa

Keywords: *copper vapour laser, dye laser, selective photoionisation, isotope separation, ^{150}Nd isotope, double beta decay, neutrino mass.*

1. Introduction

Investigation of the origin of a neutrino is one of the most important and interesting problems of fundamental physics whose solution forms our concepts about the physical world surrounding us.

A study of the double neutrinoless beta decay ($2\beta0\nu$) is one of the sources of new information about the origin of a neutrino. The rare-earth isotope ^{150}Nd (with a natural abundance of 5.6 %) is believed to be one of the most suitable materials for detecting the $2\beta0\nu$ decay, since the mass of the daughter isotope ^{150}Sm is ~ 3.3 MeV lower than the mass of the initial neodymium, and the resulting β-particles have an energy that is sufficiently high for a reliable identification and measurement of their energy. The theoretical probability of neutrinoless 2β-decay increases with transition energy and nuclear charge, and is higher for the $^{150}_{60}$Nd isotope than for $^{48}_{20}$Ca and $^{76}_{32}$Ge isotopes [1]. The expected half-life of the process $2\beta0\nu$ (if it does exist) is estimated at more than 10^{24} years; hence the minimum quantity of neodymium enriched with the ^{150}Nd isotope required for reliable measurements is 10 kg [2].

Rare-earth elements do not have volatile components convenient for isotope separation by the well-known centrifugal technique. Production of the ^{150}Nd isotope in magnetic mass separators is quite expensive. An alternative approach is to produce this isotope by the laser technique. Estimates obtained in the experiments performed in this work raise the hopes of a significant decrease in the cost of production of enriched neodymium by using the photoionisation technique.

The density of neodymium vapour attains values adequate for weight separation at evaporation temperatures of 1430 – 1530 °C. The ionisation potential of neodymium is ~ 5.5 eV. The isotope shift $\Delta\nu_{is}$ for some transitions from the lower to the first excited level in the neodymium atom is ~ 1.12 GHz. The even ^{150}Nd isotope has one unsplit individual line in the absorption spectrum. These properties of the ^{150}Nd nuclide form the basis for developing a large-scale photoionisation laser technique for producing the highly enriched ^{150}Nd isotope.

The photoionisation technique, or the atomic version of laser isotope separation (AVLIS), is based on selective photoionisation of rarefied vapour of an element by radiation from two or more lasers. The ^{150}Nd ions formed in this way are extracted from the vapour flow to a collector by applying an electric field. The rest of the atoms remain neutral, continue to move along the initial trajectory, and are trapped in the waste collectors. Since a spectrally narrow laser beam is tuned to the absorption line of one of the isotopes, separation (selection) of one isotope takes place instead of the separation of isotopes occurring in the traditional methods.

Like other methods of isotope separation, AVLIS has its own advantages and drawbacks. Let us enumerate the main highlights of this method. These include:

(i) Versatility, because almost all elements, including those without any volatile compounds, can be photoionised;

(ii) a high selectivity in a single cycle;

(iii) the possibility of purification, i.e., removal of an isotope or an element with a vanishingly small concentration in the initial mixture;

(iv) the absence of radiolysis of the working substance that allows a processing of radioactive mixtures;

(v) a high productivity per unit area of the isotope-separating unit, which makes the device compact and easy for maintenance; and

(vi) the possibility of increasing the productivity of the system simply by adding vaporising modules; in our view, this is due to the fact that the laser beam can propagate over distances of hundreds of metres without any significant deterioration of their ability to induce photoionisation.

The first theoretical works aimed at developing the technique of isotope separation by a laser beam date back to the end of 1960s [3 – 5]. This was followed by model experiments on photoionisation of rubidium [6] and uranium [7] and, finally, demonstration experiments on isotope separation of uranium [8] and calcium [9], as well as later experiments [10 – 12] carried out in laboratories of various countries. Works on selective photoionisation of isotopes of lanthanide group elements [13], in which the realisability of this process was demonstrated experimentally, are worth mentioning.

The first stage of our work on experimental implementation of laser separation of the ^{150}Nd isotope involved the designing and development of a vaporiser, vacuum module and lasers, as well as the execution of the entire working cycle starting from charging of the raw material up to the production of small quantities of isotopes in commercial form. The application of this technique for separation of ytterbium isotopes is described in detail in [12]. Apparently, the main difference between the complex of the problems being solved in our work and those considered in [12] lies in that, in view of the high natural concentration of the target ^{150}Nd sotope, contamination of the collector by the flow with natural abundance plays a comparatively minor role. This allows a considerable simplification of the system of photoion collection, which eventually leads to a significant increase in productivity.

This research was carried out under the conversion project initiated and financed by the State Research Centre 'A.I. Alikhanov Institute of Experimental and Theoretical Physics'.

2. Evaporation of neodymium

The melting point of neodymium is 1024 °C. According to [14], the expression for the saturated vapour pressure (in Pa) has the form

$$p = \exp\left(23.76 - \frac{37900}{T}\right), \quad (1)$$

where T is the temperature in kelvins. The equilibrium density of neodymium vapour at a temperature of 1400 °C is 1.3×10^{14} cm^{-3}. This temperature may serve as the starting point for designing a vaporiser.

Liquid metals are usually highly reactive and reduce even refractory metal oxides. Tantalum and tungsten virtually do not react with molten neodymium [15] and may serve as the crucible material for its evaporation. However, tantalum is an expensive metal, while massive ingots of tungsten are hard to process. Hence, a number of experimental studies aimed at finding more suitable materials were carried out on interaction of liquid neodymium with molybdenum, graphite and niobium at temperatures 1400 – 1450 °C. Molybdenum and niobium were found to be quite stable to molten neodymium [16] and were subsequently used in experiments with liquid neodymium.

Such experiments also revealed at the same time another distinguishing feature of liquid neodymium: its ability to effectively wet the metals and the creep associated with it. While wetting a material, liquid neodymium blocks the gaps between thermal screens, thus depriving them of the screening ability, which leads to a change in the thermal regime of the vaporiser. This circumstance was taken into account in the designs studied by us, and the surface creep of neodymium was reduced to the minimum possible value.

The density of atomic neodymium vapour in the region of interaction with the laser beam was measured from the absorption of a test laser beam. Such a method completely rules out the recording of dimers, clusters and drops that can be made by quartz flux meters. Figure 1 shows the experimental values of the density of neodymium vapour over a 27-cm-long vaporiser (obtained by the laser irradiation technique), theoretical values of the mean free path over the grating (which lowers the beam divergence angle γ to 60°), and the relative fraction χ_{col} of atoms undergoing collisions in 1 cm^3 of the flow over a collimating grating. The scattering of atoms from one another and from the

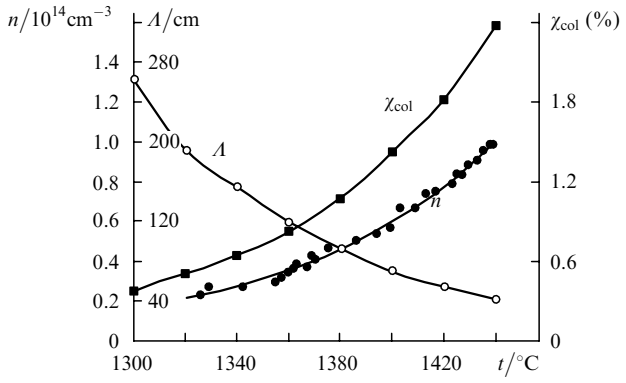

Figure 1. Experimental values of the density n of the neodymium vapour at a height of 1.5 cm over the crucible in the absence of collimating gratings, theoretical values of the mean free path Λ over the collimating grating with a 10 : 1 attenuation of the flux, and the relative fraction χ_{col} of atoms experiencing collisions in 1 cm^3 of the flow over the grating.

molecules of residual atmosphere leads to initial material dust-landing of the collector. Hence, a high concentration of the target isotope can be obtained only by lowering the density of the atoms being evaporated.

The configuration of the crucible and the evaporation temperature were varied for optimising the process. The accumulated data led to the development of a stable vaporiser with a small divergence angle of the atomic flow, an evaporation rate up to 8 g h^{-1} and an operating lifetime of 50 h.

3. Experimental facility

3.1 General configuration

The neodymium atom has an ionisation potential of 5.525 eV [17, 18] and a rich spectrum [19, 20] convenient for a three-stage photoionisation by the laser radiation in yellow–orange spectral range. Most of the laser dyes intended for operation in this wavelength range are easily excited by copper vapour lasers (CVLs), and their lasing efficiency achieves 40 % – 50 % and more. The general configuration of the experiment for such parameters of the atom being ionised is traditional and coincides with the scheme of facilities used for uranium isotope separation [21 – 23].

Figure 2 shows the general diagram of the experimental facility (without power supplies and auxiliary equipment) used in our investigations of the selective photoionisation of neodymium. A distinguishing feature of this facility is the

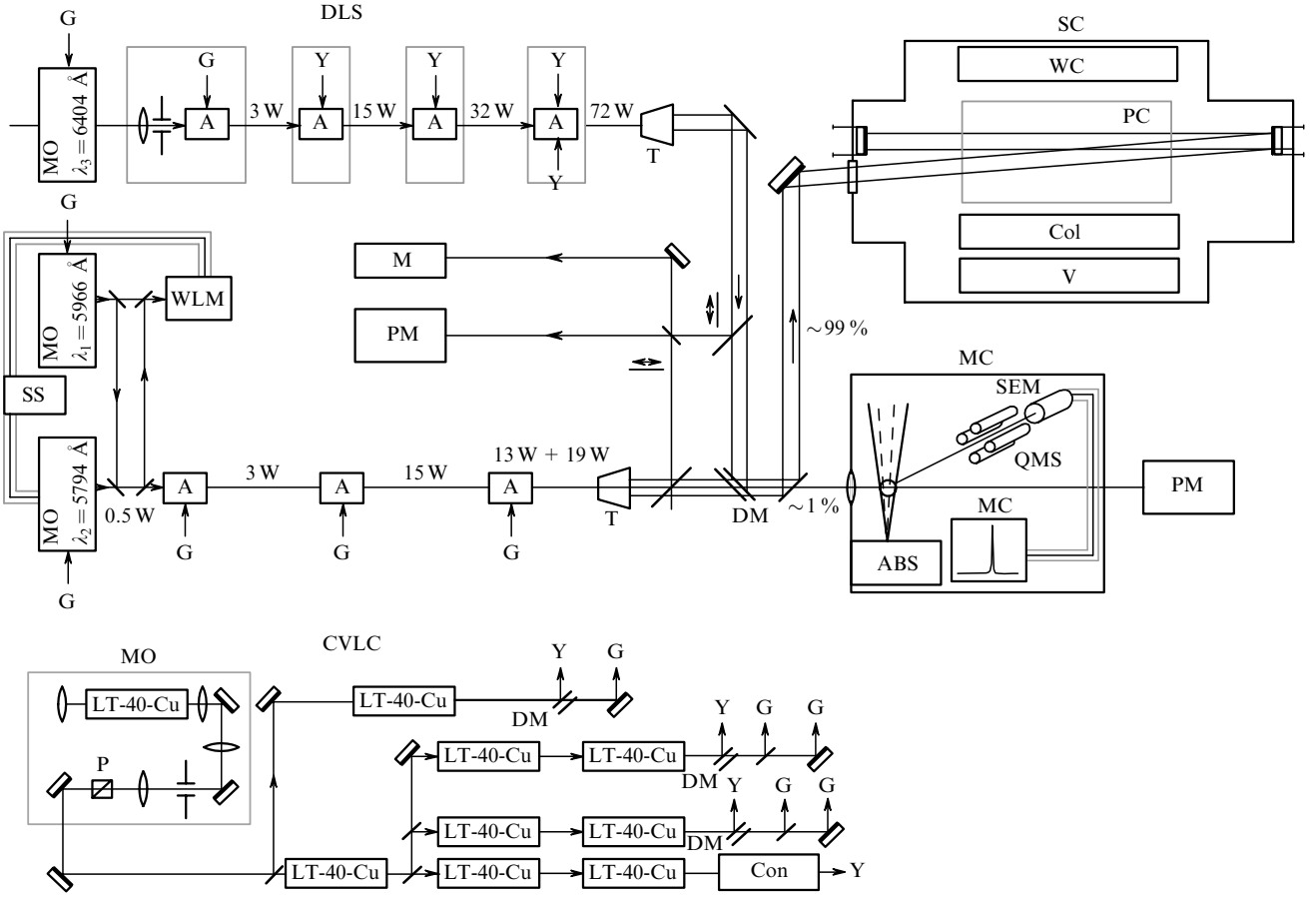

Figure 2. Schematic diagram of the experimental facility: (DLC) dye laser complex; (CVLC) copper vapour laser complex; (MC) monitor chamber; (SC) separator chamber; (MO) master oscillator; (WLM) wavelength meter; (PM) power meter; (M) monochromator; (SS) stabilisation system; (V) vaporiser; (Col) collimator; (PC) product collector; (WC) waste collector; (Y) and (G) yellow ($\lambda = 5782$ Å) and green ($\lambda = 5106$ Å) lines of the pump beam; (A) tunable dye laser amplifier; (ABS) atomic beam source; (QMS) quadrupole mass spectrometer; (SEM) secondary electron multiplier; (MS) mass spectrometer; (T) beam expander telescope; (P) polariser; (Con) converter; (DM) dichroic mirror.

presence of a monitor chamber used for recording the selectivity of purely laser action on a spectrally narrow collisionless beam of atoms during the experiment and later, at the end of the experiment, for comparing it with the selectivity obtained in the separator during operation with high atomic vapour densities and a considerable decrease in the enrichment of the isotope ^{150}Nd due to the action of deselecting processes.

For optimising the process of enrichment in the separator, the mass of the product accumulated during any experiment must be sufficient for its extraction and independent mass analysis. This condition predetermined the choice of appropriate laser powers, output capacity of the vapour source and duration of the sessions of product recovery. Mass spectrometric analysis of the obtained product was carried out in the Composition Analysis Laboratory of the Molecular Physics Institute of the Russian Research Centre Kurchatov Institute. Isotope dilution technique was used to determine the weight of the new product.

3.2 Vacuum module (separator)

The vacuum module was made of stainless steel and had a length of 125 cm for accommodating three vaporisers of length 30 cm each. The chamber was evacuated by a vapour-oil diffusion pump with a capacity of 3000 L s^{-1}.

The target isotope was extracted by an electric field produced by an electrode at a voltage of 2000–2500 V. In our experiments, the average value of the photoionic current J_{av} was $\sim 5-8$ mA for a collecting area $S_{col} = 220$ cm^2 of the collector, while the duration Δt_J of the current pulses was 20–25 μs. The fact that the recorded duration of current pulses is one-fourth of the interval $\Delta t = 100$ μs between laser shots points towards the extent of extraction being carried out. On the other hand, the completeness of extraction is also indicated by the fact that the instant current density restricted by the space charge dispersal rate, i.e.,

$$j = \frac{J_{av}}{S_{col} f \Delta t_J} \approx \frac{6.5 \times 10^{-3}\ \text{A}}{25\ \mu\text{s} \times 10^4\ \text{Hz} \times 220\ \text{cm}^2} = 0.12\ \frac{\text{mA}}{\text{cm}^2}$$

(where f is the laser pulse repetition rate) is about five times smaller than the maximum nonselective current density attained in model experiments with laser tuning under maximum photoionisation. This means that a fivefold increase in the density of ions will also result in their extraction for the same electrode voltage.

The height h (along the direction of the atomic flow) and width b (in a direction perpendicular to the atomic flow as well as the laser beam) of the working volume are chosen from the condition of maximum total irradiation of the atoms being vaporised. While the width b is determined by the construction of the vaporiser and intensity of laser beams, the value of height h depends on the velocity v of the atoms being vaporised and the laser pulse repetition rate f. Figure 3 shows the radiation probability χ_{rad} of the evaporated atoms passing through the working volume of height h, obtained as a result of averaging over the Maxwell velocity distribution with the most probable value v_p. Note that the presence of atoms exposed to two laser pulses does not indicate the possibility of repeated excitation of these atoms. In other words, the lower working level does not contain all the excited atoms that are not ionised by the instant of arrival of the second laser pulse (after 100 μs).

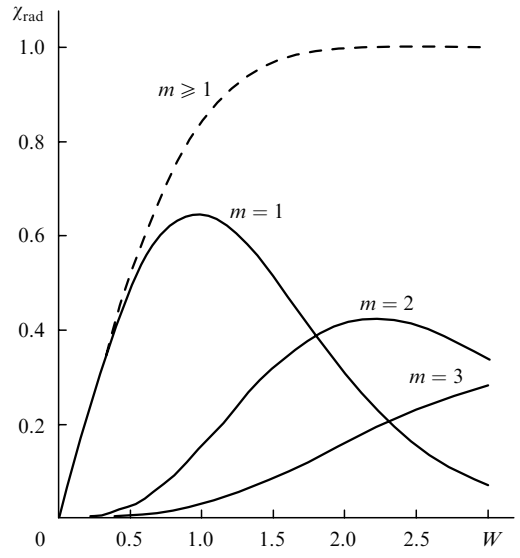

Figure 3. Probability χ_{rad} of irradiation of atoms, averaged over the Maxwell velocity distribution, as a function of the parameter $W = hf/(v_p \cos\theta_n)$, where θ_n is the angle between the direction of motion of atoms and the normal to the plane of the vapour source; m is the number of irradiations of an atom

A multipass mirror system capable of reflecting a beam up to 20 times and filling the entire working volume with light was used to cover the maximum possible vapour volume while preserving the attained values of the laser beam intensity.

3.3 Pump lasers

The pump laser complex was based on self-excited [24, 25] copper vapour emitters LT-40 Cu and thyratron modulators. CVLs were found to be very convenient pump sources for laser dyes. They have a high pulse repetition rate (10–20 kHz), a high efficiency (1 %–2 %) and a high peak power (more than 100 W) [25, 26] and are suitable for creating amplifying cascades. The total output pump power is ~ 250 W, the ratio of the intensities of green and yellow components is equal to 5/4.

A specially designed master oscillator of the CVL (Fig. 2) has a small inhomogeneity of the light spot (~ 5 %) and radiation beam divergence $\theta \leqslant 0.5$ mrad. These qualities are essential for a further effective gain in amplifier chains. A stability of ~ 0.05 mrad h^{-1} of the axis of the directional pattern of the light beam was attained which, together with the small divergence, ensures a quite stable pumping of dye lasers.

The output radiation of the pump laser complex is formed by eight LT-40 Cu amplifiers. For a laser pulse duration of ~ 30 ns, the matching in the starting time of all the amplifiers must be quite precise. The electronic system fabricated for this purpose [27] ensures the triggering of amplifiers in the amplification chains with a jitter not exceeding ± 1 ns. The average efficiency for the amplifying part of the pump laser complex was ~ 1.1 %.

The experience of operation with LT-40 Cu laser emitters reveals a high reliability and also shows that their use has a definite advantage due to the fact that the emitters are prepared in sealed form. However, the use of these emitters in amplifier chains is not quite effective. First, the windows of the LT-40 Cu emitter are prepared without an

antireflective coating and hence the loss of light even at the third amplifier becomes quite perceptible. Second, the sealed bulb of the emitter is heated strongly during operation. Heating and convection of air near the output windows lead to a distortion of the shape and instability of the position of the laser spot. These defects are removed to a considerable extent by screening the radiation beam by thin-walled metallic tubes. However, in order to improve the construction of the emitters, we prepared an open-type emitter with antireflective windows which are set on water-cooled end flanges through metallic packing. Such a construction significantly improves the quality of the laser spot and lowers the loss of light during a passage through the chain of amplifiers [28].

In order to develop a more powerful block of pump lasers, we carried out a cycle of investigations aimed at designing amplifiers with an additional power of 100–150 W. A system with circulation of the working mixture was used for a discharge channel of diameter 45 mm. The modulator constructed on the basis of two simultaneously operating TGI-2000/35 thyratrons ensured a supply of up to 12 kW power to the discharge. The working mixture had a composition $Ne + (0.5\,\% - 1.5\,\%)H_2$. For a circulation rate of 3 L min^{-1}, the output power was 92–99 W, while a small admixture of HCl ($\sim 0.5\,\%$) and an increase in the circulation rate to 12 L min^{-1} raised the output power to 166 W (for an input power of 15.5 W). It was shown that the output power and the efficiency increase with the flow rate of the buffer gas [29].

For a more complete use of the pump laser radiation, a part of the 5106-Å radiation was converted into the 5782-Å yellow line in a cell with Pyrromethene-597 [30]. Since the conversion efficiency achieved 85 %, the use of a converter with a subsequent pumping of dyes generating at 6400 Å was found to be more effective for obtaining a powerful tunable radiation in this range than the direct use of the 5106-Å line.

3.4 Tunable dye lasers

Tunable dye lasers for selective photoionisation of neodymium were constructed using a diffraction grating operating in the grazing incidence angle mode. The first transition was excited by a single-mode laser. The spectral width $\Delta\nu_{las}$ of the laser line was ~ 130 MHz, and the nonselective background pedestal intensity was $\sim 0.2\,\%$ [31, 32]. Multimode lasers with a spectral linewidth 1–2 GHz were used to excite the second and third transitions [33].

Because the generation of narrowband spectral radiation in dye lasers occurs, as a rule, with a delay of about 5–8 ns relative to the pump pulse onset, pumping of the generators was carried out by two pulses. This method allowed an equalisation of the lasing pulse and pump pulse durations, which is quite beneficial for their subsequent effective amplification [32].

Each tunable laser array contains several longitudinally pumped amplifiers [34]. This scheme allowed us to obtain high conversion efficiencies of CVL radiation into tunable radiation and to ensure a fairly uniform distribution of light intensity within the laser spot [33].

Application of quite powerful centrifugal pumps in the circulation system of laser dye solutions ensures a 2–5-fold recharging of working volume in laser cells during the interval between successive pulses. Meticulous filtering and an appropriate choice of the solvent helped improve the resistance of dye solutions to photolysis up to ~ 45 GJ $mole^{-1}$ [35].

Lasers in the third transition are pumped by the 5782-Å yellow line of the CVL (in this case, the Cresyl Violet dye is used) as well as the 5106-Å green line (with the DCM dye) (Fig. 2). The total conversion efficiency of CVL radiation into tunable radiation was $\sim 45\,\%$, while the maximum power achieved was 100 W [33].

4. Choice of photoionisation scheme

Spectra of neodymium atom have been studied widely in literature [9, 20, 36]. Information about the oscillator forces of 116 absorption lines of Nd I is contained in [36]. The efficiency of 60 versions of three-stage nonselective photoionisation of neodymium was studied in [37]. An immensely effective scheme of photoionisation of Nd I by radiation of two wavelengths $\lambda_1 = 5888$Å (~ 2.1 eV) and $\lambda_3 = 5969$Å (~ 2.07 eV) was discovered. Obviously, the energy of these two photons is insufficient for ionisation of neodymium ion and an exceptionally exact coincidence of the wavelength of the effective autoionisation transition line with one of these wavelengths is observed.

Our measurements using laser pulse delay show that the wavelengths of the second and third transitions coincide in this scheme. (If $\lambda_3 = \lambda_1$, the time delay of the pulse with λ_2 relative to the pulse with λ_1 by an amount exceeding double the laser pulse width must not lead to ionisation. Conversely, for $\lambda_3 = \lambda_2$, the time delay of the pulse with λ_2 simply leads to a slight attenuation of the ion signal due to the decay of the first excited level.)

Estimate of the isotopic shift for ^{148}Nd and ^{150}Nd at the first transition of the scheme $\Delta\nu_{is}^{(1)}(148-150) = \nu_{148} - \nu_{150}$ gives the value ~ 100 MHz, hence the main selectivity of photoionisation (Fig. 2) was attained through isotopic shift at the second transition $\Delta\nu_{is}^{(2)}(148-150) = 500$ MHz. Unfortunately, these quantities are insufficient for obtaining high ^{150}Nd concentrations in the separator chamber for vapour flows with a high density and a high divergence. The other photoionisation schemes [37], which are based on the first transition with $\lambda_1 = 5966$ Å and a relatively large isotopic shift $\Delta\nu_{is}^{(2)}(148-150)$, were not found to be very effective.

We endeavoured to look for ionisation schemes for working in the lasing zone of dyes, i.e., oxazine, phenalimine and rhodamine B. About 2000 ionisation schemes based on first transitions with $\lambda_1 = 5966$, 6288 and 6455 Å were studied. Four of these (I–IV) are singled out as the most suitable ones (Table 1). The ionisation efficiency of the new schemes was compared with the efficiency for a dichromatic scheme [37]. By way of an example, Figure 4 shows the experimental dependences of the photoionic current J on the average power density of laser radiation, which were used for selecting the most effective sequences of transitions with λ_1, λ_2 and λ_3. For calculating the intensity $\bar{I}_m$ (in W cm^{-2}) of light acting really on the atoms and

Table 1.

Scheme No	λ_1/Å	λ_2/Å	λ_3/Å
I	5966	6470	6343
II	5966	5794	6405
III	6288	5900	6491
IV	6455	6345	5855

having a nearly Gaussian distribution in time, we used the relation

$$\bar{I}_{\rm m} = \frac{\mathscr{P}}{1.5\tau_{\rm p} f}, \qquad (2)$$

where $\mathscr{P}$ is the average laser radiation power density (in W cm^{-2}); $f = 10$ kHz; and the pulse duration $\tau_{\rm p} = 22.5$ ns.

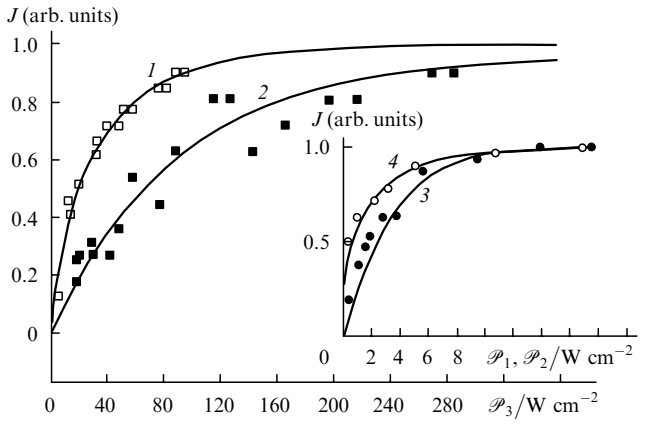

Figure 4. Dependence of the photoion current J on the average power density $\mathscr{P}_3$ of the ionising laser for a two-colour scheme with $\lambda_1 = 5889$ Å and $\lambda_2 = \lambda_3 = 5971$ Å [39] [curve (*1*)], and a three-colour scheme with $\lambda_1 = 5966.04$ Å, $\lambda_2 = 5794.17$ Å, $\lambda_3 = 6404.47$ Å for $\mathscr{P}_1 = 3.8$ W cm^{-2} and $\mathscr{P}_2 = 6.0$ W cm^{-2} [curve (*2*)]. The inset shows the dependence of the current J on the average power density of the first transition for a three-colour scheme with $\mathscr{P}_2 = 64$ W cm^{-2} and $\mathscr{P}_3 = 115$ W cm^{-2} [curve (*3*)], as well as on the average power density $\mathscr{P}_2$ of the second transition for $\mathscr{P}_2 = 23$ W cm^{-2} and $\mathscr{P}_3 = 115$ W cm^{-2} [curve (*4*)].

A comparison of the dependences of the photoionic current signals on the laser radiation intensity (Fig. 4) shows that the scheme chosen by us ($\lambda_1 = 5966.04$ Å, the first excited level energy equal to 16757.035 cm^{-1}, $\lambda_2 = 5794.17$ Å, the second excited level energy equal to 34011 cm^{-1}, and $\lambda_3 = 6404.47$ Å) is inferior to the dichromatic scheme. For example, for obtaining the photoionisation current signal equal to 0.5 of the maximum possible value, the power density in the case of scheme II (see Table 1) must be 3.5 times higher than for the dichromatic scheme. However, the isotopic shift at the first transition of this scheme $\Delta\nu_{\rm is}^{(1)}(148 - 150) \approx 1.1$ GHz allows a high selectivity of photoionisation for recovering ^{150}Nd in widely diverging dense flows of atomic vapour.

Figure 5 shows the measured dependences of the ^{150}Nd isotope concentration, obtained in the mass spectrometer of the monitor chamber, on the average laser power density for the first and second transitions. Experiments show that an increase in the laser radiation intensity at the first transition leads to a decrease in the selectivity of photoionisation. This effect was studied in detail in [38], where it is attributed to nonresonance excitation of atoms as a result of field broadening.

In the mass spectrometer of the monitor chamber, the atomic beam divergence angle γ is $\sim 5.5^\circ$. An increase in this angle leads to Doppler broadening of the absorption profile, which is one of the reasons behind the loss of selectivity during separation of ^{150}Nd. By way of an illustration of the relations between isotopic shifts, Doppler broadening and

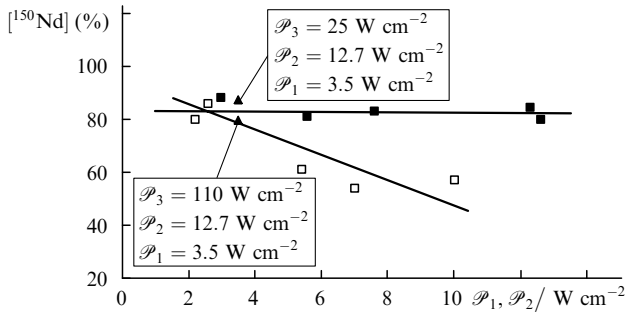

Figure 5. Dependences of the ^{150}Nd photoion concentration obtained in the mass-spectrometer of the monitor chamber for scheme II ($\lambda_1 = 5966$ Å, $\lambda_2 = 5794$ Å, $\lambda_3 = 6404$ Å) on the average power density $\mathscr{P}_1$ of the first transition for a three-colour scheme with $\mathscr{P}_2 = 3 - 5.7$ W cm^{-2} and $\mathscr{P}_3 = 92 - 108$ W cm^{-2} (□), as well as on the average power density $\mathscr{P}_2$ of the second transition for $\mathscr{P}_1 = 3.5$ W cm^{-2} and $\mathscr{P}_3 = 92 - 108$ W cm^{-2} (■). The two dark triangles show the change in the selectivity upon an increase in the average power density $\mathscr{P}_3$ of the third transition (▲).

the laser line width, Figure 6 shows the theoretical profiles of the absorption lines of even isotopes for a divergence angle $\gamma \approx 60^\circ$ for the 5966-Å line (without taking into account the field broadening) and the intensity profile of laser radiation for the first transition. The profile of the laser line shown in Fig. 6 was measured by a Troppel Model 240 Spectrum Analyser confocal scanning interferometer (with the free spectral range of 1.5 GHz and the finesse of 100) and approximated by a Gaussian profile with the FWHM $\Delta\nu_{\rm D} = 130$ MHz.

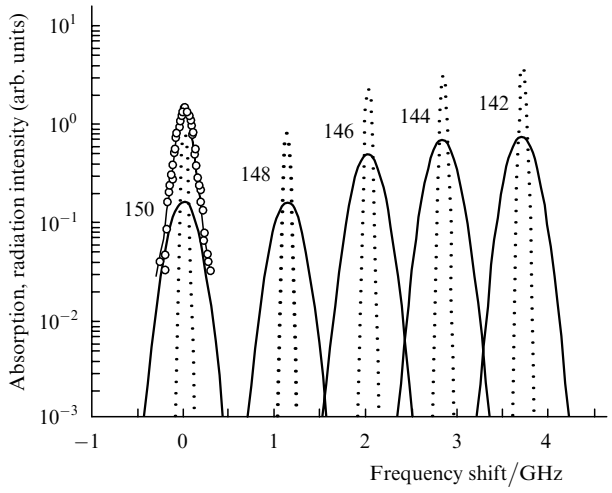

Figure 6. Theoretical profiles of the absorption lines of four isotopes for the transition at 5966 Å for a divergence angle $\gamma = 60^\circ$ (solid curves) and 5.5° (dotted curves), as well as the measured frequency dependence of laser radiation intensity for the first transition (light circles). The numbers over the curves indicate the isotope number.

The profiles of the absorption lines of even isotopes we described by the Doppler profile

$$\mathscr{D}(\Delta\nu) = \mathscr{D}(\nu - \nu_0) = \frac{2(\ln 2)^{1/2}}{\sqrt{\pi}\,\Delta\nu_{\rm D}} \times \exp\left[-4\ln 2\left(\frac{\nu - \nu_0}{\Delta\nu_{\rm D}}\right)^2\right], \qquad (3)$$

where ν_0 is the central frequency of the absorption profile. The dependence of $\Delta\nu_D$ on the divergence angle γ of the atomic flow was calculated with the help of a formula that is usually employed for molecular beams [39, 40]:

$$\Delta\nu_D(\gamma) = \Delta\nu_{D0} \sin\frac{\gamma}{2}, \tag{4}$$

where $\Delta\nu_D = \nu_0 2(\ln 2)^{1/2} v_p/c$ is the effective width of the profile (in Hz) for a random gas. To study the selectivity of photoionisation for various divergence angles γ of the atomic beam (in the direction of the laser beam), collimating gratings lowering the value of γ to 60°, 45° and 30° were installed over the vaporiser. Such experiments make it possible to determine the selectivity under the combined action of the field broadening and Doppler broadening. Experiments show that the selectivity of photoionisation increases with decreasing angle of divergence of the atomic flow [41]. A more detailed theoretical analysis of the application of collimation for narrowing the Doppler absorption profile was carried out in [42].

5. Efficiency and selectivity of the AVLIS process

5.1 External and internal parameters

In the idealised version, the productivity N_t^+ of the AVLIS process (in at. s^{-1}) for the target isotope is determined by the product of the number of target isotope atoms $N_t = \bar{n} C_{ft} C_{lev} V_{ov}$ irradiated during one pulse (in at. $pulse^{-1}$) and the probability η_t of photoionisation of these atoms and the laser pulse repetition rate (in Hz):

$$N_t^+ = N_t \eta_t f = \bar{n} L S_{rad} C_{ft} C_{lev} \eta_t f, \tag{5}$$

where $\bar{n}$ is the average density of atoms in the working volume $V_{ov} = LS_{rad}$ of the facility; S_{rad} is the overall area of the vapour region exposed to laser radiation; C_{ft} is the initial concentration of the target isotope in the irradiated mixture (here and below, the parameters for the target isotope are marked by subscript t); C_{lev} is the population of the working level at the temperature of vaporisation; and L is the length of the working volume.

Expression (5) is valid for a low pulse repetition rate f of laser pulses and a low density $\bar{n}$ of atoms, when the collector is entirely free from the dust of scattered atoms. We define the parameter β as the fraction of the flux of atoms F entering the separating cell, which falls on the photoionic collector as a result of atomic collisions. The coefficient β exhibits a complex dependence on the design of the separating cells, angle of divergence γ of the atomic flow and the number of collisions suffered by the atoms during their passage through the part of the working volume from which direct trajectories to the collector are possible [43].

Note that a very high working density $\bar{n}$ of neutral atoms may lead to a considerable loss of ions of the target isotope in the case of resonance charge transfer. As an example, let us estimate the probability χ_{ctr} of neodymium ions avoiding charge transfer with intrinsic neutral atoms for a density $\bar{n} \approx 10^{12}$ cm^{-3}. According to [14, 44], the dependence of the resonance charge transfer cross section σ_{ctr} of neodymium atoms on their velocity v_{ion} can be described by the semiempirical expression

$$\sigma_{ctr}^{1/2} = 2.14 a_0 \ln\frac{c}{v_{ion}}, \tag{6}$$

where $a_0 = 0.53 \times 10^{-8}$ cm. For a width $b = 4$ cm of the vapour flow for an ion having a thermal velocity $\bar{v}_{ion} = 500$ m s^{-1} at a temperature 1430 °C, the probability of resonance charge transfer over a path of length $l = (2/3)b$ is defined as

$$\eta_{ctr} = \bar{n}\sigma_{ctr} l = 10^{12} \times 2.7 \times 227 \times 10^{-16} = 6.1 \times 10^{-2}. \tag{7}$$

The fraction χ_{ctr} of the target isotope atoms escaping charge transfer is found to be ~ 0.94. Note that this estimate was obtained by using the thermal velocity of an ion before its acceleration in the electric field of the extractor, i.e., the minimum value of χ_{ctr} was obtained.

Let us now write down the detailed expressions for the product flux P and the concentration C_{pt} of the target isotope in it. The product flux (in g h^{-1}) is defined as

$$P = \left[FC_{lev}\left(C_{ft}\eta_t^s + \sum_i C_{fi}\eta_i^s\right)\chi_{rad}\chi_{ex} + \beta F\right]\chi_{att}$$

$$= (I + D)\chi_{att}, \tag{8}$$

where F (in g h^{-1}) is the feed flux; the coefficient χ_{att} is introduced to take into account the possibility of photoions rebounding from the collector after incidence at its surface, as well as of the ionic sputtering of the recovered material, and characterises the product deposition efficiency; χ_{ex} is the fraction of photoions extracted from the flow by the electric field of the collector; I is the ion flux enriched with the target isotope; and D is the neutral component flux at the collector with the initial isotopic concentration; here and below, the summation over i indicates summation over all nontarget isotopes (this means six neodymium isotopes with mass numbers 148, 146, 145, 144, 143, 142). We introduce into the flux I the part I_t corresponding to the target isotope alone:

$$I_t = FC_{lev}C_{ft}\chi_{rad}\chi_{ex}\eta_t^s. \tag{9}$$

In this case, the concentration of the target isotope in the product at the collector is defined as

$$C_{pt} = \frac{FC_{lev}C_{ft}\eta_t^s\chi_{rad}\chi_{ex}\chi_{ctr} + \beta C_{ft}F}{P/\chi_{att}}$$

$$= \frac{\chi_{ctr} I_t + C_{ft} D}{I + D}. \tag{10}$$

The ionisation probabilities for the separator in expressions (8)–(10) are indicated by the superscript s. In the following analysis, we shall use the ionisation probability for the separator (η^s) and in the monitor chamber (η^m), which differ only in that the width of the Doppler profiles of the isotopes is ~ 70 MHz, while its value in the separator is 300 MHz and higher.

The following parameters are usually employed for describing the efficiency of the separation process in the isotope separation technique:
separation factor

$$\alpha = \frac{C_p/(1 - C_p)}{C_w/(1 - C_w)}, \tag{11}$$

selectivity

$$S^* = \frac{C_p/(1-C_p)}{C_f/(1-C_f)}, \tag{12}$$

and the coefficient of extraction of the target isotope from the feed flux

$$\Psi = \frac{PC_p}{FC_p}, \tag{13}$$

where C_w is the concentration of the target isotope in the waste. The parameters χ_{ctr}, χ_{rad} and χ_{ex} can be measured or evaluated theoretically with a fairly high degree of precision. However, the three internal parameters η_t^s, $\overline{\eta_{nt}^s} = \sum_i C_{fi}\eta_i^s / \sum_i C_{fi}$ and β, which are extremely important for optimising the enrichment process, cannot be estimated directly from the measurement of six external parameters: the feed flow F, the product flow P, and the waste flow W, as well as the concentrations C_f, C_p and C_w of the target isotope in them.

5.2 Determination of the concentration of target isotope photoions in the separator and other internal parameters

We introduce the parameters C_{ph}^m and C_{ph}^s for the primary concentration of photoions formed by laser radiation in the monitor chamber and the separator respectively:

$$C_{pht}^m = \frac{C_{ft}\eta_t^m}{C_{ft}\eta_t^m + \sum_i C_{fi}\eta_i^m},$$
$$C_{pht}^s = \frac{C_{ft}\eta_t^s}{C_{ft}\eta_t^s + \sum_i C_{fi}\eta_i^s}. \tag{14}$$

Usually, the experimental conditions are chosen in such a way that $\chi_{ex} = 1$. Hence, by using definitions (9) and (14), we can write the following expression for the primary flux of photoions of the target isotope

$$I_t = FC_{lev}C_{ft}\chi_{rad}\eta_t^s = C_{pht}^s I$$

or, for any other isotope

$$I_i = C_{phi}^s I. \tag{15}$$

The expression for the concentration (10) of the product can now be presented in the following form:

$$C_{pt} = \frac{\chi_{ctr}C_{pht}^s I + C_{ft}D}{I+D},$$

whence

$$\chi_{ctr}C_{pht}^s = \frac{C_{pt}(I/D+1) - C_{ft}}{I/D}. \tag{16}$$

We have retained the notation C_{pt} for the target isotope concentration. However, formula (16) is of more general nature and is applicable for any isotope i since the concentrations C_{pi} и C_{fi} in the product and feed flows can be measured for it. Thus, the values of C_{phi}^s are determined by the measurable quantities C_{pi} and C_{fi}, as well as the ratio I/D which is the same for all isotopes and is common for our experiment.

When the laser is tuned to the isotope ^{150}Nd, the ratio C_{phi}^m/C_{fi} decreases rapidly with the mass of the isotope (i.e., with increasing isotope shift $\Delta\nu_{isi}^{(1)} = \nu_{150} - \nu_i$). This can be seen clearly from the values of the ionisation efficiency $\eta_i^m \cdot \text{const} = C_{phi}^m/C_{fi}$ for even isotopes shown in Table 2. We introduce the ratio $\alpha_i = C_{phi}^s/C_{phi}^m$ which is more than unity for non-target even isotopes (with the exception of the case $\Delta\nu_D^m = \Delta\nu_D^s$). For the masses of the isotopes 146–142, the function $\alpha_i = f(\Delta\nu_{isi}^{(1)})$ varies weakly, and hence

$$\alpha_{146} \approx \alpha_{144} \approx \alpha_{142}, \quad \frac{\alpha_{i+2}}{\alpha_i} \approx 1. \tag{17}$$

Let us write the expression for α_{i+2}/α_i in the case of isotopes ^{142}Nd and ^{144}Nd, substituting for C_{phi}^s its values obtained by using (16):

$$\frac{\alpha_{142}}{\alpha_{144}} = \frac{C_{ph\,142}^s}{C_{ph\,142}^m}\frac{C_{ph\,144}^m}{C_{ph\,144}^s} = \frac{C_{ph\,144}^m}{C_{ph\,142}^m}\frac{C_{p\,142}(I/D+1) - C_{f\,142}}{C_{p\,144}(I/D+1) - C_{f\,144}} \approx 1. \tag{18}$$

The ratio I/D can be determined by equating the right-hand side of (18) to unity. For example, we can write for sample No. 76 (Table 2)

$$\frac{I}{D} = \frac{C_{ph\,144}^m C_{f\,142} - C_{ph\,142}^m C_{f\,144}}{C_{ph\,144}^m C_{p\,142} - C_{ph\,142}^m C_{p\,144}} - 1 = 4.801 - 1 = 3.801. \tag{19}$$

Table 2.

Isotope	C_{fi} (%)	C_{phi}^m (%)	C_{phi}^m/C_{fi}	Sample No. 75		Sample No. 76		Sample No. 77		Sample No. 78		Sample No. 79		$\bar{C}_{phi}$ (%)
				experiment	theory	experiment	theory	experiment	theory	experiment	theory	experiment	theory	
				C_{pi} (%)	C_{phi}^s (%)	C_{pi} (%)	C_{phi}^s (%)	C_{pi} (%)	C_{phi}^s (%)	C_{pi} (%)	C_{phi}^s (%)	C_{pi} (%)	C_{phi}^s (%)	
^{150}Nd	5.6	91.58	16.35	34.1 ± 0.2	70 ± 2	56.3 ± 0.2	71 ± 2	35.3 ± 0.2	73 ± 2	16.5 ± 0.2	73 ± 4	9.6 ± 0.2	71 ± 9	71.8
^{148}Nd	5.7	4.59	0.805	11.1 ± 0.2	18 ± 1	16.3 ± 0.2	19 ± 1	10.9 ± 0.2	18 ± 1	7.7 ± 0.2	18 ± 1	6.4 ± 0.2	17 ± 2	18.0
^{146}Nd	17.2	2.61	0.152	12.9 ± 0.2	7.4 ± 0.2	9.3 ± 0.2	7.1 ± 0.2	12.5 ± 0.2	7.0 ± 0.2	15.4 ± 0.2	6.0 ± 0.5	16.6 ± 0.2	7.3 ± 2	6.8
^{145}Nd	8.3	0.27	0.0325	5.4 ± 0.2	1.7 ± 0.2	3.0 ± 0.2	1.5 ± 0.2	5.2 ± 0.2	1.3 ± 0.2	7.2 ± 0.2	1.5 ± 0.3	7.9 ± 0.2	1.7 ± 1	1.5
^{144}Nd	23.8	0.86	0.0344	14.2 ± 0.2	2.4 ± 0.5	6.4 ± 0.2	1.3 ± 0.5	13.9 ± 0.2	1.4 ± 0.5	20.1 ± 0.2	1.0 ± 1	22.5 ± 0.2	2 ± 2	1.4
^{143}Nd	12.2	0.03	0.00246	7.0 ± 0.2	0.4 ± 0.3	2.9 ± 0.2	0.3 ± 0.1	7.0 ± 0.2	0.4 ± 0.3	10.3 ± 0.2	0.5 ± 0.5	11.5 ± 0.2	1 ± 1	0.4
^{142}Nd	27.2	0.08	0.00294	15.3 ± 0.2	0.1 ± 0.1	5.8 ± 0.2	0.1 ± 0.1	15.2 ± 0.2	0.1 ± 0.1	22.8 ± 0.2	0.1 ± 0.1	25.6 ± 0.2	0.1 ± 0.1	0.1

Note: $\bar{C}_{phi}$ is the theoretical value of C_{phi}^s averaged over all samples; the following values were used in calculations $I/D = 0.78 \pm 0.03$ (sample No. 75), 3.7 ± 0.2 (No. 76), 0.79 ± 0.03 (No. 77), 0.19 ± 0.01 (No. 78) и 0.065 ± 0.005 (No. 79).

The value of I/D averaged over several points was found to be equal to 3.7. Further, according to (16), we obtain in the case $C_{\mathrm{p}\,150} = 0.563$ the following expression for $C^{\mathrm{s}}_{\mathrm{ph}\,150}$

$$\chi_{\mathrm{ctr}} C^{\mathrm{s}}_{\mathrm{ph}\,150} = \frac{C_{\mathrm{p}\,150}(3.7+1) - C_{\mathrm{p}\,150}}{3.7} = 0.70. \qquad (20)$$

The values of $C^{\mathrm{s}}_{\mathrm{ph}\,i}$ obtained by averaging over several measurements are presented in Table 2.

The efficiency of the method proposed here was verified in a special experiment in which samples for mass-spectrometric analysis were taken from regions with quite different dustings on the appropriately prepared collector. Table 2 shows the results of our experiments and calculations of the primary concentration of photoions in the separator. It follows from the data presented in the table that in spite of the specially created complication (the dusting fluxes varied by a factor of 57), the average value of $C^{\mathrm{s}}_{\mathrm{ph}\,i}$ were determined for even isotopes with an error of 5 % – 10 %, which is admissible for subsequent estimation.

As an example, let us calculate the inner parameters for $C_{\mathrm{pt}} = 0.563$, $P = 6.1$ mg h^{-1}, $F = 1410$ mg h^{-1}, $\chi_{\mathrm{ctr}} = 0.94$, $\chi_{\mathrm{rad}} = 0.9$, $\chi_{\mathrm{att}} = 0.6$, $\chi_{\mathrm{ctr}} C^{\mathrm{s}}_{\mathrm{ph\,t}} = 0.7$, and $I/D = 3.7$. Substituting $I = 3.7D$ into (10), we arrive at the expression

$$C_{\mathrm{pt}} = 0.563 = \frac{3.7D\,\chi_{\mathrm{ctr}} C^{\mathrm{s}}_{\mathrm{ph\,t}} + 0.056D}{P/\chi_{\mathrm{att}}} = \frac{2.65D}{10.17},$$

which gives $D = 2.16$ mg h^{-1}. Since $P/\chi_{\mathrm{att}} = I + D$, we obtain $I = 8.01$ mg h^{-1}. In turn, the flux of the target isotope at the collector is given by

$$\frac{PC_{\mathrm{pt}}}{\chi_{\mathrm{att}}} = \chi_{\mathrm{ctr}} I_{\mathrm{t}} + C_{\mathrm{ft}} D = 5.72 \text{ mg h}^{-1},$$

which gives $I = 5.96$ mg h^{-1}. Further, the total photoion flux of non-target isotopes is given by

$$I_{\mathrm{nt}} = I - I_{\mathrm{t}} = 2.05 \text{ mg h}^{-1}.$$

We can now determine the internal parameters $\eta^{\mathrm{s}}_{\mathrm{t}}$, $\overline{\eta^{\mathrm{s}}_{\mathrm{nt}}}$ and β easily. Since $I_{\mathrm{t}} = FC_{\mathrm{lev}} C_{\mathrm{ft}} \chi_{\mathrm{rad}} \eta^{\mathrm{s}}_{\mathrm{t}}$, we obtain

$$\eta^{\mathrm{s}}_{\mathrm{t}} = \frac{5.96}{1410 \times 0.0293} = 0.145.$$

It follows from the equality $I_{\mathrm{nt}} = FC_{\mathrm{lev}} C_{\mathrm{f\,nt}} \chi_{\mathrm{rad}} \overline{\eta^{\mathrm{s}}_{\mathrm{nt}}}$ that

$$\overline{\eta^{\mathrm{s}}_{\mathrm{nt}}} = \frac{2.05}{1410 \times 0.493} = 0.00295.$$

The dusting coefficient is defined as

$$\beta = \frac{D}{F} = \frac{2.16}{1410} = 0.00153.$$

Thus, for isotope separation of elements containing several even isotopes whose spectra are separated by distances larger than the spectral width of the absorption profile of the atomic beam used in the investigations, we can calculate the internal parameters required for designing the production unit.

5.3 Direct measurements of the photoionisation probability

One of the most important internal parameters determining the efficiency of the AVLIS process is the probability η_{t} of photoionisation of the target isotope. In this connection, we carried out direct measurements of the photoionisation probability. The experimental setup is shown schematically in Fig. 7. The working volume analogous to that used in the separator chamber was organised in the vacuum chamber of diameter 50 cm directly over the vaporiser forming a weakly diverging beam (with a divergence angle of 2°). The working volume contains a photoion collector under a voltage of about −50 V and a grounded deflector. The collector is used for extracting photoions from the atomic flow. A multipass optical system ensures repeated passage of a laser beam of diameter 1 cm, the length of the zone exposed to radiation being 9 cm in the direction of atomic flow, which corresponds to an irradiation probability ~ 0.95 (see Fig. 3). Neodymium atoms that were not ionised by light as a result of interaction with the laser beam continue their rectilinear motion and reach the ion source of the quadrupole mass spectrometer. The distance between the photoionisation region and the mass spectrometer is 25 cm, and the average time of flight is 0.6 ms. The atoms can be registered by the mass spectrometer in two ways: by the electron impact method and as a result of photoionisation by laser radiation branching off from the main laser beam.

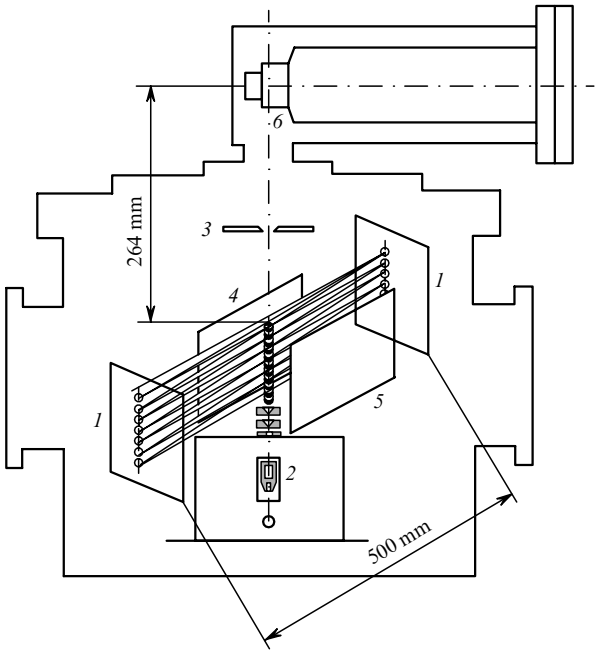

Figure 7. Scheme of the experiment on measurement of photoionisation probability: (*1*) multipass system; (*2*) vaporiser; (*3*) diaphragm; (*4*) deflector; (*5*) collector; (*6*) mass spectrometer.

The experimental technique can be described as follows. The mass filter of the mass spectrometer is tuned to the target isotope (to increase the sensitivity of the method, the experiment was carried out for the ^{142}Nd isotope, which has the highest natural abundance of 27 %). The laser wavelengths are tuned to the photoionisation peak of the target isotope. Exposure of the atomic beam to laser radiation in the working volume leads to a partial photoionisation of the target isotope, while an attenuation of the signal propor-

tional to the photoionisation probability is observed in the mass spectrometer during testing of the irradiated atomic flux.

When atoms are detected by the electron impact technique in the mass spectrometer, the ratio of the difference between signals for closed and open laser radiation in the working volume to the signal for closed laser radiation gives the decrease in the amount of target isotope as a result of photoionisation. Since the atoms were excited from the ground state, the probability of photoionisation is determined by dividing this value by the equilibrium population density of the ground state, which is equal to 0.58 at the evaporation temperature.

When laser photoionisation is used for registering atoms in the mass spectrometer, only atoms of the target isotope that are in the ground state are detected. Hence, the decrease in the signal caused by opeing the laser radiation in the working volume is proportional to the extent to which the ground state is depleted.

Experiments performed out using schemes of photoionisation by radiation with $\lambda_1 = 5966.04$ Å, $\lambda_2 = 5794.17$ Å and $\lambda_3 = 6404.47$ Å. For average power densities $\mathscr{P}_1 \sim 0.5$ W cm^{-2}, $\mathscr{P}_2 \sim 0.5$ W cm^{-2} and $\mathscr{P}_2 \sim 39$ W cm^{-2}, a photoionisation probability of 0.70 ± 0.06 and a depletion coefficient ~ 0.9 of the ground state were obtained. Note that spatial overlapping of beams corresponding to successive passes took place in the working volume. For a small separation (~ 50 cm) between the mirrors of a multipass system, this leads to superposition of pulses, and the atoms are exposed to laser radiation with a double intensity on the average.

By using the obtained value of the depletion coefficient of the ground state, we can estimate the photoionisation probability. The main channel of the loss of excited atoms is the decay of the second excited state with a time constant $\tau_2 = 40$ ns [45]. Most of the atoms disintegrate into metastable states that do not participate in the photoionisation process. The number of atoms leaving the second excited state per unit time due to disintegration and photoionisation is proportional to $1/\tau_2 + W_{23}$, where

$$W_{23} = \frac{\bar{I}_m \sigma_3}{h\nu_3} \tag{21}$$

is the frequency (in Hz) of transitions to the autoionisation state; $\bar{I}_m$ (in W cm^{-2}) and $h\nu_3$ (in J) are the intensity and energy of an ionising radiation quantum; and σ_3 (in cm^2) is the cross section of the ionising transition.

For a photoionisation cross section $\sigma_3 = 2 \times 10^{-16}$ cm^2 and intensity $\bar{I}_m = 2.4 \times 10^5$ W cm^{-2} corresponding to an average power density $\mathscr{P}_3 \sim 80$ W cm^{-2}, the frequency of transitions to the autoionisation state $W_{23} = 150$ MHz and is much higher than the reciprocal of the laser pulse duration $1/25$ ns $= 40$ MHz. In this case, the fraction of atoms departing from the second excited state to the autoionisation state can be estimated as $W_{23}/(1/\tau_2 + W_{23}) = 0.86$. In order to estimate the probability of photoionisation, the obtained value should be multiplied by the depletion coefficient of the ground state. As a result, the probability η_t of photoionisation of the target isotope is found to be $0.86 \times 0.9 = 0.77$, which is approximately in accord with the measured probability.

Thus, as a result of passage of atoms through the working volume in the experiment considered here, the probability η_t of photoionisation of the target isotope is found to be ~ 0.7, the probability of the atom remaining in the ground state is about 0.1, and the probability of its being in the metastable state during decay of the second excited level is equal to 0.15–0.2.

6. Results of experiments on the recovery of neodymium enriched by the ^{150}Nd isotope, and discussion

Usually, the duration of such experiments was about 1 h. The vaporisation temperature and diameters of the laser beams as well as the collimating gratings, collector configuration, etc. were varied in order to obtain the maximum productivity for a sufficiently high level of isotope enrichment. Table 3 shows the results of the most successful experiments. The technique developed in the previous sections was used to estimate the inner parameters of the isotope separation process for each experiment.

The experimentally obtained quantity of the product is found to be smaller than the value calculated from the photoionic current because of an incomplete deposition of photoions on the collector as well as ionic sputtering of the extracted product. The efficiency χ_{att} of deposition of the product on the collector was estimated from the material balance equation using the amount of the target isotope ^{150}Nd at the electrode opposite to the collector, i.e., the deflector.

The value $\chi_{att} = 0.6$ in Table 3 was used for all experiments, although this quantity could change slightly due to a variation of the structure and position of the collector. Marginal losses of the product during washing from the

Table 3.

Experiment No.	Conditions of Experiment				External parameters			Theoretical parameters		Separator fluxes			Internal parameters		
	Collector part	H/ cm	d/ mm	Z	P/ mg h^{-1}	C_{pt} (%)	F/ mg h^{-1}	I/D	$\chi_{ctr}C_{ph\,150}$ (%)	D/ mg h^{-1}	I/ mg h^{-1}	P/χ_{att}/ mg h^{-1}	η_t^s	$\overline{\eta_{nt}^s}$	$\beta = D/F$
	Lower	30	30	18	11.1	42.2		1.39	68.5	7.8	10.8	18.5			1.9×10^{-3}
1	Upper	30	30	18	9.8	53.7		2.15	76.1	5.2	11.1	16.3			1.3×10^{-3}
	Entire collector				20.9	47.6	4002			12.9	21.9	34.8	0.14	3.1×10^{-3}	3.2×10^{-3}
	Lower	30	30	18	10.8	65.8		4.21	80.1	3.5	14.6	18.0			9.8×10^{-4}
2	Upper	30	30	18	5.4	53.4		2.37	73.6	2.7	6.3	9.0			7.6×10^{-4}
	Entire collector				16.2	61.7	3534			6.1	20.9	27.0	0.16	2.6×10^{-3}	1.7×10^{-3}
3	Entire collector	15	20	25	18.1	58.3	4284	2.17	82.6	9.5	20.7	30.2	0.14	1.7×10^{-3}	2.2×10^{-3}
4	Entire collector	15	20	25	16.5	64.4	3734	3.33	82.0	6.4	21.2	27.5	0.16	2.1×10^{-3}	1.7×10^{-3}
5	Entire collector	30	20	25	42.7	60.1	8018	2.52	82.0	20.3	51.0	57.7	0.18	2.3×10^{-3}	2.5×10^{-3}

Note: H is the effective size of the collector; d is the laser beam diameter; Z is the number of passes.

collectors, which were cleaned thoroughly before each experiment for erasing the isotope memory, were also not taken into account in Table 3.

The laser power density in our experiments varied in the following range: $\mathscr{P}_1 = 1.5 - 2.5$ W cm^{-2}, $\mathscr{P}_2 = 2.5 - 6$ W cm^{-2}, $\mathscr{P}_3 = 10 - 20$ W cm^{-2}. It can be seen from Table 3 that the real recovery P of the product (determined by measuring the amount of the product washed off the collector) varied from 15 to 43 mg h^{-1} for a vaporiser of length $l = 27$ cm and target isotope concentrations $C_{pt} = 50\,\% - 65\,\%$ The ionisation efficiency η_t^s of the target isotope for 18–25 passages of the laser beam was $\sim 0.11 - 0.18$, which is much lower than the value (0.7) attained in special experiments described above (see Sec. 5). This raises hopes of a better extraction of the target isotope in a production unit employing more powerful ionising radiation.

When the working volume in our experiments was filled by light, laser beams could pass through the same place once, twice, or even thrice. For estimates, we assume that the average number of passes is equal to two. In this case, the ionisation probability η_t^s per pass is $\sim 0.055 - 0.09$.

Obviously, the productivity of the facility can be increased not only by increasing the average power density $\mathscr{P}_3$ of the ionising radiation, but also by modernising the extractor with a view to decrease the losses associated with the sputtering of the product due to ion bombardment. The inclusion of the first metastable state with a population density $C_{lev} \approx 26\,\%$ at a temperature of $\sim 1430\,^\circ$C in the ionisation system can also make a significant contribution.

The cycle of works on laser enrichment of ^{150}Nd allows us to explore the possibilities of obtaining weighted amounts of this isotope and to evaluate the results of experiments on extraction of enriched neodymium as well the cost of the process. For a 0.6 probability of photoionisation of the target isotope in the separator and involvement of atoms at the first metastable level into photoionisation process, about 50 kg of the isotopic product can be obtained during 6000 working hours on a device of length 10 m. In principle, there are no obstacles in this process: laser radiation can propagate over distances of 100 m and more, while vacuum modules can be easily connected with one another to form a unified system of the required size. The fact that a considerable part of the apparatus was constructed in our laboratory and that the experiments were carried out over a long time makes it possible to estimate the capital expenditures and operational cost of producing a sample of mass 50 kg. The cost of the product is found to be 5–7 times lower than for ^{150}Nd enriched by the electromagnetic method.

7. Conclusions

Our experience of the ^{150}Nd enrichment by the laser technique has shown that, like all other methods of isotope separation, productivity and selectivity are mutually exclusive factors and a delicate optimisation of experimental conditions is required for attaining the desired results. A method is proposed for evaluating the internal parameters that are of fundamental importance for optimising the process. The probability of photoionisation in a collimated atomic beam is measured directly. It is shown in the experiments that the probability of photoionisation of even isotopes may attain values up to 0.7.

The obtained results and their reliable reproducibility lead to the expectation that laser technique can be used for isotope separation of rare-earth elements that do not have any volatile compounds.

According to our estimates, the cost of the process of laser separation of ^{150}Nd is much lower than in the case when magnetic mass separators are used for this purpose.

8. References

1. Artem'ev V.A., Brakhman E.V., Vasil'ev S.I., et al. *Yadern. Fiz.*, **59** (1), 10 (1996).
2. Elliot S.R., Vogel P. *Ann. Rev. Nucl. Part. Sci.*, **52**, 115 (2002).
3. Kudrin L.P., Novikov V.M., Blinkin V.L. *Metody razdeleniya izotopov osnovannye na selektivnom fotovozbuzhdenii* (Isotope Separation Methods Based On Selective Photoexcitation) (IAE-1968 report); *Russian Research Centre Kurchatov Institute booklet* (Moscow, 2002) p. 39.
4. Letokhov V.S. *O vozmozhnosti razdeleniya izotopov metodami rezonansnoi fotoionizatsii atomov i fotodissoctsiatsii molekul lazernym izlucheniem* (On the Possibility of Isotope Separation by Methods Based on Photoionisation of Atoms and Photodissociation of Molecules by Laser Radiation) (FIAN-1969 report); Preprint No. 1, Institute of Spectroscopy, USSR Academy of Sciences (Moscow, 1979) p. 1.
5. Letokhov V.S. Author's certificate No. 784679. Priority from 30.03.70. *Bull. Izobret.*, No. 18, 308 (1982).
6. Ambartsumyan R.V., Kalinin V.N., Letokhov V.S. *Pis'ma Zh Eksp. Teor. Fiz.*, **13**, 305 (1971).
7. Roussel C. *Production d'une Vapeur d'Uranium et Interaction Avec un Rayonnement Infra-Ronge*. Dissertation a l'Universite Scientifique et Medicale de Grenoble (Grenoble, 1972).
8. Tussio S.A., Durbin J.W., Peterson O.G., et al. *IEEE J. Quantum Electron.*, **10** (9), 790 (1974).
9. Brinkman U., Hartig W., Telle H., Walther H. *Appl. Phys.*, **5**, 109 (1974).
10. Janes J.S., Izkan I., Pike C.T. *IEEE J. Quantum Electron.*, **12** (2), 111 (1976).
11. Karlov N.V., Krynetskii B.B., Mishin V.A., et al. *Kvantovaya Elektron.*, **3** (11), 2486 (1976) [*Sov. J. Quantum Electron.*, **6**, 1363 (1976)].
12. Tkachev A.N., Yakovlenko S.I. *Kvantovaya Elektron.*, **33**, 581 (2003) [*Quantum Electron.*, **33**, 581 (2003)].
13. Karlov N.V., Krynetskii B.B., Mishin V.A. Preprint FIAN No. 48 (Moscow, 1977).
14. Grigoriev I.S., Meilikhov E.Z. (Eds) *Fizicheskie velichiny. Spravochnik* (Handbook of Physical Quantities) (Moscow: Energoatomizdat, 1991) pp 1232.
15. Savitskii E.M., Terekhova V.F. *Metallovedenie redkozemel'nykh metallov* (Metallurgy of Rare-earth Metals) (Moscow: Nauka, 1975).
16. Grigoriev A.I., Grigoriev I.S., Kovalevich S.K., et al., in *Proc. of the III All-Russian (International) Conf. on Physicochemical Processes in Selection of Atoms and Molecules* (Zvenigorod: Central Research Institute TsNIIatominform, 1998) p. 64.
17. Kikoin I.K. (Ed.) *Tablitsy fizicheskikh velichin* (Tables of Physical Quantities) (Moscow: Atomizdat, 1976) p. 302.
18. Radtsig A.A., Smirnov B.M. *Parametry atomov i atomnykh ionov. Spravochnik* (Handbook of Parameters of Atoms and Atomic Ions) (Moscow: Enegoatomizdat, 1986).
19. Martin W.C., Zalubas R., Hagan L. *Atomic Energy Levels. The Rare-Earth Elements* (Washington, National Bureau of Standards, 1978, NSRDS-NBS) Vol. 60.
20. Van Leeuwen K.A.H., Eliel E.R., Post B.H., et al. *Zeitschrift fur Physik A – Atoms and Nuclei*, **301**, 95 (1981).
21. *Laser Applications: Isotope Separation* (Livermore: Lawrence Livermore National Laboratory, 1984) TB-067.
22. Bass I.L., Bonanno R.E., Hackel R.P., et al. *Appl. Opt.*, **31**, 6993 (1992).
23. Greenland P.T., Travis D.N., Wort D.J.H. *J. Phys. B: At. Mol. Opt. Phys.*, **24**, 2945 (1990).

24. Isaev A.A., Kazaryan M.A., Petrash G.G. *Pis'ma Zh. Eksp. Teor. Fiz.*, **16** (1), 40 (1972).
25. Belyaev V.P., Zubov V.V., Isaev A.A., et al. *Kvantovaya Elektron.*, **12**, 74 (1985) [*Sov. J. Quantum Electron.*, **15**, 40 (1985)].
26. Batenin V.M., Buchanov V.V., Kazaryan M.A. *Lazery na samoogranichennykh perekhodakh atomov metallov* (Self-contained Metal Atom Lasers) (Moscow: Izd-vo Nauchnaya kniga, 1998).
27. Firsov V.A., Suslov V.I., Belousov A.B., et al., in *Proc. of the VI All-Russian (International) Conf. on Physicochemical Processes in Selection of Atoms and Molecules* (Zvenigorod: Central Research Institute TsNIIatominform, 2002) pp 235–239.
28. Grigoriev A.I., Grigoriev I.S., Dorovskii A.P., et al., in *Proc. of the III All-Russian (International) Conf. on Physicochemical Processes in Selection of Atoms and Molecules* (Zvenigorod: Central Research Institute TsNIIatominform, 1999) pp 91–92.
29. Grigoriev A.I., Grigoriev I.S., Kovalevich S.K., et al., in *Proc. of the Symposium on Metal Vapour Lasers* (Sochi, 2002).
30. D'yachkov A.B., Kovalevich S.K., in *Proc. All-Russian (International) Conf. on Physicochemical Processes in Selection of Atoms and Molecules* (Zvenigorod: Central Research Institute TsNIIatominform, 2002) pp 256–259.
31. D'yachkov A.B., Kovalevich S.K., Pesnya A.V., et al., in *Proc. of the IV All-Russian (International) Conf. on Physicochemical Processes in Selection of Atoms and Molecules* (Zvenigorod: Central Research Institute TsNIIatominform, 2000) p. 120.
32. Grigoriev I.S., Dyachkov A.B., Kuznetzov V.A., et al. *Proc. SPIE Int. Soc. Opt. Eng.*, **5121**, 411 (2003).
33. Grigoriev I.S., Dyachkov A.B., Labozin V.P., et al. *Kvantovaya Elektron.*, **34**, 447 (2004) [*Quantum Electron.*, **34**, 447 (2004)].
34. D'yachkov A.B., Labozin V.P., in *Proc. of the V All-Russian (International) Conf. on Physicochemical Processes in Selection of Atoms and Molecules* (Zvenigorod: Central Research Institute TsNIIatominform, 2001) p. 132.
35. Dyachkov A.B., Labozin V.P. *Kvantovaya Elektron.*, **32**, 825 (2002) [*Quantum Electron.*, **32**, 825 (2002)].
36. Blaise J., Chevillard J., Verges J., et al. *Spectrochimica Acta B*, **25**, 333 (1970).
37. Zyuzikov A.A., Mishin V.I., Fedoseev V.N. *Opt. Spektr.*, **64** (3), 480 (1988).
38. Grigoriev I.S., Dyachkov A.B., Labozin V.P., et al., in *Proc. of the VI All-Russian (International) Conf. on Physicochemical Processes in Selection of Atoms and Molecules* (Zvenigorod: Central Research Institute TsNIIatominform, 2002) p. 188.
39. Zaidel' A.N., Ostrovskaya G.V., Ostrovskii Yu.I. *Tekhnika i praktika spektroskopii* (Technology and Practice of Spectroscopy) (Moscow: Nauka, 1976).
40. Ramsay N. *Molecular Beams* (Oxford: Oxford Univer. Press, 1956; Moscow: Inostrannaya Lit., 1960).
41. Kovalevich S.K., Labozin V.P., Tsvetkov G.O. *Zh. Tekh. Fiz.*, **75** (1), 98 (2005).
42. Yakovlenko S.I., in *7 Zababakhinskie nauchnye chteniya* (7th Zababakhin Research Reports) (Snezhinsk, 2003).
43. Maiorov S.A., Tkachev A.N., Yakovlenko S.I. *Matem. Model.*, **6** (9), 13 (1994).
44. Smirnov B.M. *Asimptoticheskie metody v teorii atomnykh stolknovenii* (Asymptotic Methods in the Atomic Collisions Theory) (Moscow: Atomizdat, 1973).
45. D'yachkov A.B., Kovalevich S.K., Labozin V.P., et al., *in Proc. of the VIII All-Russian (International) Conf. on Physicochemical Processes in Selection of Atoms and Molecules* (Zvenigorod: Central Research Institute TsNIIatominform, 2004) p. 64.